Modeling conduction in electron waveguides with finite-range impurities

Hoshik Lee, Han Hsu, and L. E. Reichl
Center for Studies in Statistical Mechanics and Complex Systems, The University of Texas at Austin, Austin, Texas 78712, USA
(Received 3 August 2004; published 11 January 2005)

We study the conductance of an electron waveguide with a finite range impurity using reaction matrix theory. We compute the scattering matrix for the waveguide and use it to obtain an exact expression for the Landauer conductance. In an effort to simplify the computation of conductance in such systems, we review the convergence difficulties that occur if δ-function impurities in two space dimensions are used in place of finite range impurities. We compare our exact result for the waveguide conductance with a finite range impurity with the case of the δ-function impurity with the finite number of modes. We determine conditions for which a δ-function impurity can be used to approximate the conductance when a finite range impurity is present.

DOI: 10.1103/PhysRevB.71.045307 PACS number(s): 05.60.Gg, 73.23.Ad, 73.50.Bk

I. INTRODUCTION

There is considerable interest in modeling the effect of impurities on electron flow in GaAs/AlGaAs electron waveguides.[1] Models involving a single impurity inside a waveguide have been discussed by Bagwell[2] and by Boese *et al.*[3,4] The combined effect of the impurity potential and backscattering off the walls of the quantum waveguide can give rise to quasibound states and resonance behavior and thereby have an important effect on the conductivity. The use of delta functions to model finite range impurity potentials is very attractive because they can simplify considerably the computations necessary to obtain the conductivity in the presence of impurities. However, as noted in Refs. 4 and 5, δ-functions in two or more space dimensions have convergence problems. Because of these convergence problems, some authors have resorted to the use of more complicated potentials such as, for example, the impurity D function in Ref. 6 or a one-dimensional δ-function for one space dimension and a finite sized potential (a Gaussian) along the other space dimension.[4] However, as we will see, under certain conditions it is possible to use δ-function potentials to model the effects of finite range impurities on the conductivity of electron waveguides.

We are particularly interested in the effects of impurities on the conductance of semiconductor based two-dimensional (2D) electron waveguides or carbon nanotubes. For this reason we restrict our discussion to electron flow in two space dimensions. The problem of convergence occurs for all types of boundary conditions in 2D space. In all cases, in order to approximate a finite range potential by a δ-function potential, we must introduce a cutoff on the modes. For completeness, in Sec. II, we show how to approximate a finite range potential in open space by a δ-function potential, and in Sec. III, we consider the conditions under which a finite range potential confined inside a hard wall container (a closed system) can be approximated by a δ-function potential. In Sec. IV, we focus on the effect of finite range and δ-function impurities on the conductivity of a two-dimensional electron waveguide. This last case is the most difficult because we must compare the conductance of the waveguide when a δ-function impurity is present with the conductance when a finite range impurity is present. In order to calculate the conductance of a waveguide with a finite range impurity, we first calculate S-matrix by using reaction matrix theory. We then calculate the conductance with the δ-function impurity and compare our results with that obtained for the finite range impurity. Finally, in Sec. V we make some concluding remarks.

II. THE DELTA-FUNCTION IMPURITY IN 2D OPEN SPACE

The Hamiltonian operator for a single electron of mass m_e in two dimensional open space, in the presence of a δ-function potential located at the origin, can be written

$$\hat{H} = \frac{\hat{p}^2}{2m_e} + V_0\delta^2(\hat{\mathbf{r}}) = E, \tag{1}$$

where $\hat{p}$ and $\hat{\mathbf{r}}$ are the momentum and position operators, respectively, of the electron, E is the total energy, and V_0 is the strength of the δ-function potential. The energy Green's function for this system can be written

$$G(\mathbf{r}_1,\mathbf{r}_2) = \langle \mathbf{r}_1 | \frac{1}{E\hat{1} - \hat{H}} | \mathbf{r}_2 \rangle = G_0(\mathbf{r}_1,\mathbf{r}_2) + \frac{V_0 G_0(\mathbf{r}_1,\mathbf{0}) G_0(\mathbf{0},\mathbf{r}_2)}{1 - V_0 G_0(\mathbf{0},\mathbf{0})}, \tag{2}$$

where $G_0(\mathbf{r}_1,\mathbf{r}_2)$ is the free particle energy Green's function

$$G_0(\mathbf{r}_1,\mathbf{r}_2) = \langle \mathbf{r}_1 | \frac{1}{E\hat{1} - \hat{H}_0} | \mathbf{r}_2 \rangle \tag{3}$$

and $H_0 = \hat{p}^2/2m_e$. If the δ-function potential is attractive, $V_0 < 0$, we expect that a single bound state exists and the bound state energy is given by a pole of the Green's function. The condition for the pole is $1 - V_0 G_0(\mathbf{0},\mathbf{0}) = 0$. In two space dimensions, this can be written in the form

$$\frac{1}{\lambda} = -\frac{1}{2\pi}\int_0^\infty \frac{k}{k^2 - B} dk, \tag{4}$$

where $E_B = \hbar^2 B/2m_e$ is a bound state energy and is negative and $\lambda = 2m_e V_0/\hbar^2$. If we integrate the right-hand side of Eq. (4), it diverges even though the left hand side has a finite

value. Thus, in two space dimensions a bound state does not exist as long as the strength of δ-potential V_0 is finite. In a scattering problem, the *s* wave scattering amplitude is undefined for $V_0 \neq 0$.[7]

We can resolve this difficulty by introducing a cutoff, Λ, on the upper limit of the integration in Eq. (4). In other words, if we integrate from 0 to Λ rather than from 0 to ∞, we can obtain a bound state energy, *B*, given by

$$B = -\Lambda^2 e^{(2\hbar^2\pi/m_e V_0)}. \tag{5}$$

Let us now compare this to the bound state energy in a cylindrical potential of finite radius, *a*. The Hamiltonian is

$$H = -\frac{\hat{p}^2}{2m_e} + U(r) = E, \tag{6}$$

where the potential is

$$U(r) = V_0/\pi a^2, \quad \text{if } 0 < r < a \text{ and } U(r) = 0 \text{ if } r > a. \tag{7}$$

The potential, $U(r)$, becomes a two-dimensional δ function in the limit, $a \to 0$. If we solve the Schrödinger equation, $H\psi_E = E\psi_E$, assuming that the wave function, ψ_E, and its first derivative are continuous at the surface of cylinder, we obtain the bound state energy,

$$E_B = -\frac{2\hbar^2 e^{-2\gamma}}{m_e a^2} e^{(2\hbar^2\pi/m_e V_0)}, \tag{8}$$

where γ is a Euler constant ($\gamma = 0.577$). If we compare Eq. (5) and (8), and require that the δ-function potential give the same bound state energy as the cylinder, we can find that the momentum cutoff Λ is inversely proportional to the radius a of the impurity potential.

III. DELTA-FUNCTION IMPURITY IN A CLOSED SYSTEM

For a 2D closed system containing finite range impurity, we can use the energy eigenstates of the impurity-free system as an orthonormal basis with which to compute the eigenstates and eigenvalues of the system when the impurity is present. This basis set contains an infinite (countable) number of states, but in practice we generally can use only a finite number of the basis states to compute physical quantities such as energy eigenvalues to get convergent results. However, this is not true for the case of a δ-function impurity in the closed system where the values of physical quantities vary with mode number and never converge. However, we can use the δ-function impurity to approximate an impurity with specified range, *a*, if we use a finite number of modes, N_t. We will show that N_t and *a* can be related explicitly.

Let us consider an electron confined in a 2D circular potential well with an infinitely hard wall and radius *R* in the presence of a repulsive delta-function impurity that lies at the center of the circular well. The Schrödinger equation for this system, in cylindrical coordinates, can be written

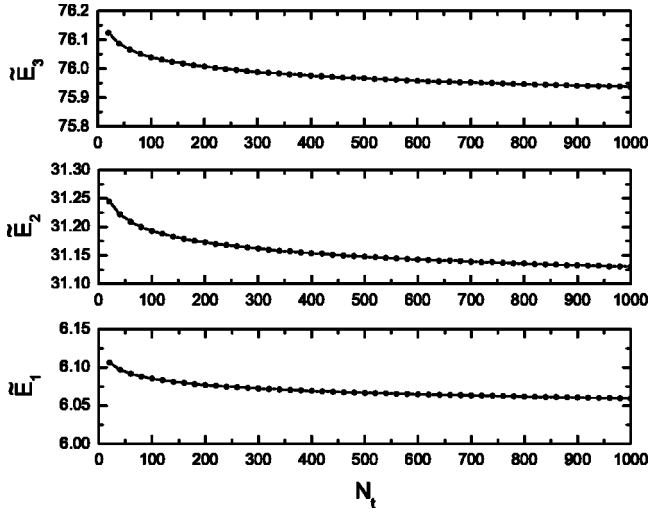

FIG. 1. The lowest three energy eigenvalues of a circular potential well, with a δ-function impurity at the center, are plotted as a function of the number N_t of modes. Energies decrease approximately logarithmically with N_t and do not converge.

$$-\frac{\hbar^2}{2m_e}\left(\frac{\partial^2}{\partial r^2} + \frac{1}{r}\frac{\partial}{\partial r} + \frac{\partial^2}{\partial \phi^2}\right)\psi(r,\phi) + V(r)\psi(r,\phi) = E\psi(r,\phi), \tag{9}$$

where $V(r) = V_o\delta(r)/2\pi r$ for $r < R$ and $V(r) = \infty$ for $r > R$. When the δ-function impurity lies at the center of the circle, only states with zero angular momentum need to be considered. For states with nonzero angular momentum, the wave function vanishes at $r = 0$, and is not affected by the delta function potential. Energy eigenstates, $\psi_E(r)$, with zero angular momentum can be expanded in Bessel functions as

$$\psi_E(r) = \sum_{n=1}^{\infty} \frac{A_n}{R\sqrt{\pi}J_1(x_{0n})} J_0\left(x_{0n}\frac{r}{R}\right), \tag{10}$$

where J_ν is the Bessel function of order ν and x_{0n} is the *n*th zero of $J_0(x)$. If we substitute Eq. (10) into Eq. (9), use the orthonormality of Bessel functions and interchange $n' \leftrightarrow n$, we obtain the following equation for coefficients A_n:

$$x_{0n}^2 A_n + \frac{2m_e V_o}{\hbar^2\pi}\frac{1}{J_1(x_{0n})}\sum_{n'=1}^{\infty}\frac{A_{n'}}{J_1(x_{0n'})} = \frac{2m_e R^2 E}{\hbar^2}A_n. \tag{11}$$

In practice, when we solve Eq. (11) for A_n and the energy eigenvalues, *E*, the total number of equations for A_n must be truncated to a finite value N_t. It is quite natural to expect the eigenvalues to converge to some value as N_t increases, but that does not occur. To see this, let us consider the case where $\tilde{V}_o = V_o/(\pi\hbar^2/2m_e) = 0.1$. In Fig. 1, we plot the three lowest (dimensionless) energies ($\tilde{E} = E/(\hbar^2/2m_e R^2)$), $\tilde{E}_1$, $\tilde{E}_2$, and $\tilde{E}_3$ for different values of N_t. None of them converge to any specific values but decrease approximately logarithmically with increasing values of N_t.

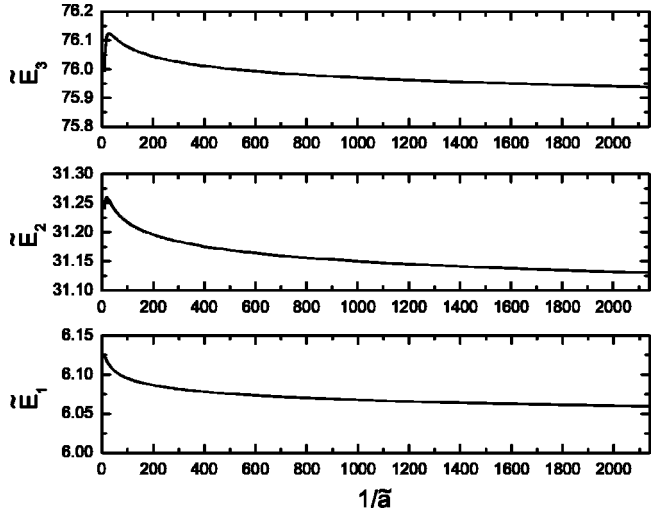

FIG. 2. The lowest three energy eigenvalues of a circular potential well with a finite size impurity at the center are plotted as functions of the impurity size. The eigenenergies decrease with $1/\tilde{a}$ for small $\tilde{a}$ in a manner similar to their dependence on N_t in Fig. 1. The dip in eigenenergies at very small $1/\tilde{a}$ occurs because the electron effectively no longer sees the impurity at small $1/\tilde{a}$.

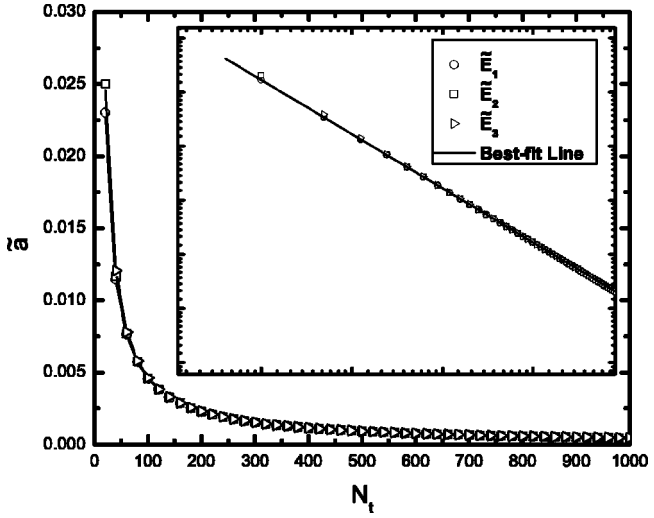

FIG. 3. The relation between the number of modes N_t and impurity size $\tilde{a}$. The inset is plotted on a log scale. For all energies, $\tilde{a}$ and N_t satisfy the relation $\tilde{a}=0.46\times(1/N_t)$.

Let us now find the energy eigenvalues of an electron confined in a 2D circular potential well with a finite range impurity at the center. The potential, $V(r)$ now has the form $V(r)=V_o/\pi a^2$ for $0<r<a$, $V(r)=0$ for $a<r<R$ and $V(r)=\infty$ for $r>R$. Note that $V(r)\rightarrow V_o\delta(r)/2\pi r$ for $r<R$ as $a\rightarrow 0$. Therefore, we will concentrate on the case of $a\ll R$. We consider states with zero angular momentum in order to compare with the case of δ-function impurity. The eigenstates with zero angular momentum are $\psi_E(r)=I_o(\kappa r)$ for $0<r<a$ and $\psi_E(r)=AJ_o(kr)+BN_o(kr)$ for $a<r<R$, where $I_o(x)$, $J_o(x)$, and $N_o(x)$ are Bessel functions, $\kappa^2=(2m_eV_o/\pi\hbar^2a^2)-(2m_eE/\hbar^2)$ and $k^2=(2m_eE/\hbar^2)$. By requiring $\psi_E(r)=0$ at $r=R$ and requiring the continuity of the wave function and its derivative at $r=a$, we obtain

$$\kappa\frac{I_1(\kappa a)}{I_o(\kappa a)}=-k\frac{J_1(ka)N_o(kR)-J_o(kR)N_1(ka)}{J_o(ka)N_o(kR)-J_o(kR)N_o(ka)}. \qquad (12)$$

Using Eq. (12), energy eigenvalues $\tilde{E}_i$ $(i=1,2,3)$ for various impurity ranges a are computed. In Fig. 2, we show the relationship between $\tilde{E}_i$ and $\tilde{a}=a/R$ with $\tilde{V}_o=0.1$. We can see that the energies $\tilde{E}_i$ decrease with $1/\tilde{a}$ for small $\tilde{a}$ in a manner similar to $\tilde{E}_i$ versus N_t in Fig. 1. It is interesting to note that unlike Fig. 1, $\tilde{E}_i$ has a sudden dip at very small $1/\tilde{a}$, which can be seen most clearly for the case of $\tilde{E}_3$ versus $1/\tilde{a}$ in Fig. 2. The dip occurs because for small $1/\tilde{a}$ the impurity fills the cylindrical well and the particle effectively sees only the cylindrical well. This cannot occur for the delta-potential impurity.

Let us next determine the range of the impurity $\tilde{a}$ that allows the finite impurity system to have the same energy eigenvalues as the δ-function impurity system truncated to N_t basis states for the case $\tilde{V}_0=0.1$. The relation between $\tilde{a}$ and N_t is plotted in Fig. 3. We see that a smaller total number of eigenmodes N_t corresponds to a greater range of the impurity $\tilde{a}$ as we would expect. By plotting $\tilde{a}=a/R$ and N_t on a log scale the relation between $\tilde{a}$ and N_t emerges clearly. For all energy eigenvalues, they can be fitted to the relation $\log\tilde{a}=-0.78-1.00\log N_t$, or equivalently $\tilde{a}=0.46\times(1/N_t)$. Thus, the impurity range is inversely proportional to total number of eigenmodes, N_t. As mentioned before, this relation is valid only for sufficiently small $\tilde{a}$ or, equivalently, large N_t (in this case, $\tilde{a}<0.02$ or $N_t>20$).

To see how the relation between $\tilde{a}$ and N_t changes with the strength of the potential $\tilde{V}_o$, we introduce a parameter μ such that $1/\mu=N_t\tilde{a}=N_t(a/R)$, where R, the radius of the circular area, is a measure of the length scale of the region of confinement. We find that for $\tilde{V}_o=0.1$, $\mu=2.17$, while for $\tilde{V}_o=10$, $\mu=2.32$. As we change the strength of the impurity by two orders of magnitude, the parameter μ only changes by about 10%. In other words, μ depends only weakly on the strength of the impurity. This implies that for a given system, a particular truncation of N_t modes corresponds approximately to a particular impurity size, no matter how strong the impurity is.

IV. THE CONDUCTANCE FOR SINGLE IMPURITY IN A 2D WAVEGUIDE

A single impurity inside a two-dimensional electron waveguide can have a large effect on the conductance of the waveguide because it can cause electron localization and resonances. Using a two-dimensional δ-function simplifies considerably the calculation of the Green's function for a waveguide system. However, as is shown in Ref. 4, the conductance found by this method does not converge as mode number is increased. In this section, we compare the conductance of a 2D quantum waveguide with a finite range impurity to its conductance with a δ-function impurity, and we

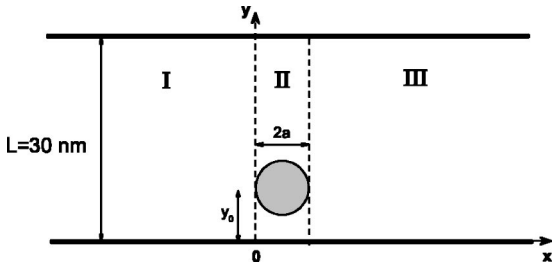

FIG. 4. The geometry of the two-dimensional electron waveguide with a single disk shaped impurity. L is the width of the waveguide. a is the radius of the impurity and y_0 is the transversal position of the impurity. I and III denote the asymptotic regions and II denotes the reaction region.

determine conditions under which the system with the δ-function impurity can be used to approximate the system with the finite range impurity.

The conductance of a 2D waveguide with a finite range impurity is complicated to calculate. However, Akguc and Reichl[8] have shown how to calculate the S-matrix for complicated (chaotic) waveguide systems using the reaction matrix theory proposed by Wigner and Eisenbud.[9] In the subsections below, we first introduce the reaction matrix theory for the scattering matrix of the waveguide and then use the results to obtain the conductance in the presence of a finite range impurity. We then compare this with the conductance when a δ-function impurity is present.

A. Reaction-matrix

Let us consider electron flow in a 2D waveguide. To be specific we consider a waveguide formed from GaAs semiconductor material. We assume the width of waveguide is $L=300$ Å and the mass of the electron is $m^*=0.067m_e$, where m_e is the mass of a free electron and m^* is the effective mass of an electron in GaAs/AlGaAs.

The Schrödinger equation for a single electron in the 2D electron waveguide shown in Fig. 4 is given by

$$\left[-\frac{\hbar^2}{2m^*}\left(\frac{\partial^2}{\partial x^2}+\frac{\partial^2}{\partial y^2}\right)+V_c(y)+V_I(x,y)\right]\Psi(x,y)=E\Psi(x,y), \tag{13}$$

where $V_c(y)$ is the potential that confines an electron in the waveguide and $V_I(x,y)$ represents the impurity potential. For simplicity we assume the waveguide has infinitely hard walls so $V_c(y)=\infty$ for $y\leqslant 0$ or $y\geqslant L$ and $V_c=0$ for $0<y<L$. The impurity potential is a disk shaped barrier of radius a and centered at $(x=x_o,y=y_o)$. Thus, $V_I(x,y)=g/\pi a^2$ for $x=x_o+r\cos(\phi),y=y_o+r\sin(\phi)$ for $r<a$ and $0\leqslant\phi\leqslant 2\pi$, and $V_I(x,y)=0$ otherwise. Here g is a constant, r is the distance from the center of the impurity, and ϕ is the azimuthal angle measured about the center of the impurity.

As shown in Fig. 4, we divide the waveguide into left and right asymptotic regions and a reaction region which contains the impurity. The wave function in the reaction region is expanded in a complete orthonormal set of basis states, $\phi_j(x,y)$, which are essentially the eigenstates of a billiard with the finite range impurity centered at (x_o,y_o). The states are zero at the waveguide walls $y=0$ and $y=L$ and they have zero slope at the interfaces $x=0$ and $x=2a$. The eigenvalues associated with these eigenfunctions are denoted λ_j. The states $\phi_j(x,y)\equiv\langle x,y|\phi_j\rangle$ can be expanded in the form

$$\phi_j(x,y)=\sum_{p=1}^{\infty}\sum_{q=0}^{\infty}B_{pq}^{j}\sqrt{\frac{2}{L}}\sin\left(\frac{p\pi y}{L}\right)M_q\cos\left(\frac{q\pi x}{2a}\right), \tag{14}$$

where B_{pq}^{j} are the expansion coefficients and $M_q=\sqrt{1/2a}$ for $q=0$ while $M_q=\sqrt{1/a}$ for $q\neq 0$.

The wave functions in the asymptotic regions, $x<0$ and $x>2a$, are expanded in complete sets of states, $\Phi_n^{\alpha}(x,y)$, where $\alpha=l(r)$ denote left (right) asymptotic regions. The states $\Phi_n^{\alpha}(x,y)$ are zero at the waveguide walls $y=0$ and $y=L$. Therefore, the states $\Phi_n(x,y)$ have the form

$$\Phi_n^{\alpha}(x,y)\equiv\langle x,y|\Phi_n^{\alpha}\rangle=\sqrt{\frac{2}{L}}\chi_n^{\alpha}(x)\sin\left(\frac{n\pi y}{L}\right). \tag{15}$$

The final results of the computation will be independent of the choice of boundary conditions at the interfaces.[10]

As shown in Refs. 11 and 12, the energy eigenstates $\langle x,y|E\rangle$ of the waveguide can be expressed in the form

$$\langle x,y|E\rangle=\sum_{j=1}^{\infty}\gamma_j\phi_j(x,y)+\sum_{\alpha=r,l}\sum_{n=1}^{\infty}\Gamma_n^{\alpha}\Phi_n^{\alpha}(x,y). \tag{16}$$

We require that the wave function $\langle x,y|E\rangle$ be continuous at the interfaces. The continuity of energy eigenstates, at the interfaces between the reaction region and asymptotic regions, gives us

$$\Gamma_n^{\alpha}\chi_{k_n}^{\alpha}(x_\alpha)=\sum_{n'=1}^{\infty}R_{\alpha l}(n,n')\left.\frac{d\chi_{k_{n'}}^{l}}{dx}\right|_{x_l}\Gamma_{n'}^{l}-\sum_{n'=1}^{\infty}R_{\alpha r}(n,n')\left.\frac{d\chi_{k_{n'}}^{r}}{dx}\right|_{x_r}\Gamma_{n'}^{r}, \tag{17}$$

where

$$R_{\alpha\beta}(n,n')=\frac{\hbar^2}{2m^*}\sum_{j=1}^{\infty}\frac{\phi_{j,n}(x_\alpha)\phi_{j,n'}(x_\beta)}{E-\lambda_j} \tag{18}$$

is the (n,n')th matrix element of the reaction matrix. The quantity, $\phi_{j,n}(x_\alpha)$, is a measure of the overlap between the jth reaction region state and nth transverse mode in the asymptotic regions. It is defined

$$\phi_{j,n}(x_\alpha)=\sqrt{\frac{2}{L}}\int_0^{\infty}dy\,\phi_j(x_\alpha,y)\sin\left(\frac{n\pi y}{L}\right), \tag{19}$$

where $x_l=0$ and $x_r=2a$.

We must distinguish between propagating modes and evanescent modes in the asymptotic regions of the waveguide. The propagating modes are given by

$$\Gamma_n^l \chi_{k_n}^l(x) = \frac{a_n^p}{\sqrt{k_n}} e^{ik_n x} - \frac{b_n^p}{\sqrt{k_n}} e^{-ik_n x} \text{ for } x < 0,$$

$$\Gamma_n^r \chi_{k_n}^r(x) = \frac{c_n^p}{\sqrt{k_n}} e^{ik_n x} - \frac{d_n^p}{\sqrt{k_n}} e^{-ik_n x} \text{ for } x > 2a, \tag{20}$$

where the wave vector k_n is

$$k_n = \sqrt{\frac{2m^* E}{\hbar^2} - \left(\frac{n\pi}{L}\right)^2}. \tag{21}$$

If there are m propagating modes then $n=1,2,\ldots,m$. The evanescent modes ($(n\pi/L)^2 > 2m^* E/\hbar^2$) are given by

$$\Gamma_n^l \chi_{k_n}^l(x) = -\frac{b_n^e}{\sqrt{k_n}} e^{\kappa_n x} \text{ for } x < 0,$$

$$\Gamma_n^r \chi_{k_n}^r(x) = -\frac{d_n^e}{\sqrt{k_n}} e^{-\kappa_n x} \text{ for } x > 2a, \tag{22}$$

where

$$\kappa_n = \sqrt{\left(\frac{n\pi}{L}\right)^2 - \frac{2m^* E}{\hbar^2}}. \tag{23}$$

For evanescent modes, the index $n=m+1,m+2,\ldots,\infty$.

B. The scattering matrix

In order to construct the scattering matrix for this system, we substitute Eqs. (20) and (22), into Eq. (17) and then we rewrite the matrices which involve evanescent modes in terms of matrices which involve propagating modes (see Appendix). All matrices involving evanescent modes in the Appendix are infinite dimensional since there are an infinite number of evanescent modes. However, for finite range impurities only a finite number of evanescent modes need be kept to obtain and accurate expression for the *S*-matrix. The number of propagating modes is determined by the Fermi energy. As shown in the Appendix, we can obtain the following expression for the $2m \times 2m$ *scattering matrix* (*S*-matrix):

$$\overline{\mathbf{S}} = U^\dagger \frac{\mathbf{1_p} - i\widetilde{\mathbf{Z}}}{\mathbf{1_p} + i\widetilde{\mathbf{Z}}} U^\dagger = \begin{pmatrix} \overline{r} & \overline{t'} \\ \overline{t} & \overline{r'} \end{pmatrix} \tag{24}$$

where $\overline{t}$ and $\overline{t'}$ are $m \times m$ matrices of transmission probability amplitudes and $\overline{r}$ and $\overline{r'}$ are $m \times m$ matrices of reflection probability amplitudes. The matrices $\widetilde{\mathbf{Z}}$ and $U^\dagger$ are $2m \times 2m$ matrices defined in the A, and $\mathbf{1_p}$ is $m \times m$ identity matrix.

C. The conductance for waveguide with finite range impurity

The electron conductance G in the waveguide is given by the Landauer's formula and can be expressed in terms of the transmission amplitudes t_{ij} as

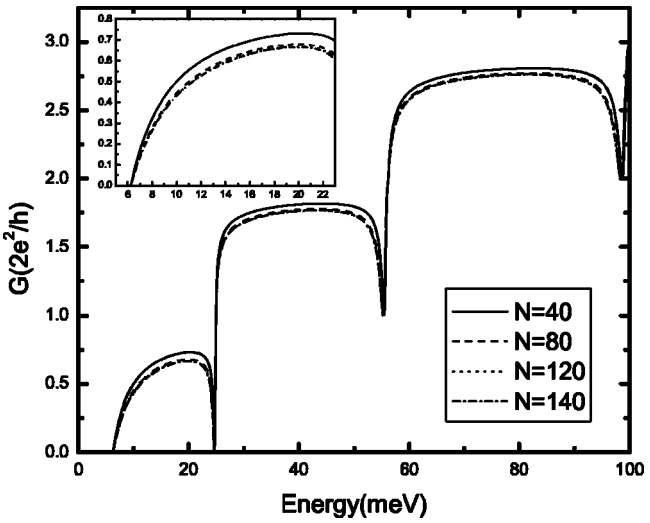

FIG. 5. Conductance of a waveguide with a finite range impurity for different numbers of modes, N. The impurity is disk shape, the potential strength $g=-7$ feV cm^2, and the radius $a=L/150$. When using $N=120$, the conductance has converged to its final result. Just before the opening of the $(n+1)$th channel, the transmission amplitude $t_{n,n}$ goes to zero. These transmission dips only occur for attractive impurities and involve an alignment of the impurity size and the decay length $1/\kappa_{n+1}$.

$$G = \frac{2e^2}{h} \sum_{i,j}^{m} |t_{ij}|^2, \tag{25}$$

where the e is the electron charge, h is Planck's constant, and the sum extends over all propagating modes. The transmission amplitudes are determined from the expressions in Sec. IV B. In our calculations, we locate the center of the impurity at $x_o=a$ and $y_o=5L/12$, and we choose $a=L/150$ and $g=-7$ feV cm^2. We consider an attractive impurity here. Figure 5 shows the electron conductance for a waveguide with a finite range impurity, for different total numbers of modes, N (N includes for propagating and evanescent modes). Because of the finite size of the impurity, we obtain convergent results when we use large enough number of modes ($N=120$ in this case). In Fig. 6, the solid line shows the conductance for $N=120$ and the dashed line is the conductance of a straight waveguide without an impurity present. From Fig. 6, we see that the impurity induces resonance and a considerable decrease in the conductance relative to the case when no impurity potential is present. Just before the threshold for the $(n+1)$th channel opening, the transmission probability amplitude, $t_{n,n}$, goes to zero. This only occurs for attractive impurities and for incident energies such that the inverse wave vector $1/\kappa_{n+1}$ becomes of order of the impurity size.[2,3].

D. The conductance for waveguide with delta-function impurity

Let us now compute the conductance when a δ-function impurity is present at $(x_o=0, y_o=5L/12)$ (this case was also considered in Refs. 2 and 3). The Green's function for this system is

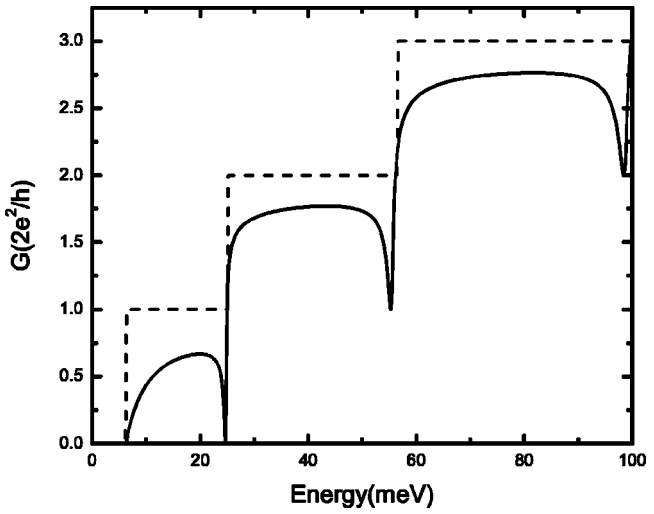

FIG. 6. Comparison of the conductance of a waveguide with finite range impurity and a waveguide with no impurity. The solid line is for the waveguide with a disk shaped impurity with $g=-7$ feV cm^2, $N=120$, and $a=L/150$. The dotted line is for the waveguide with no impurity.

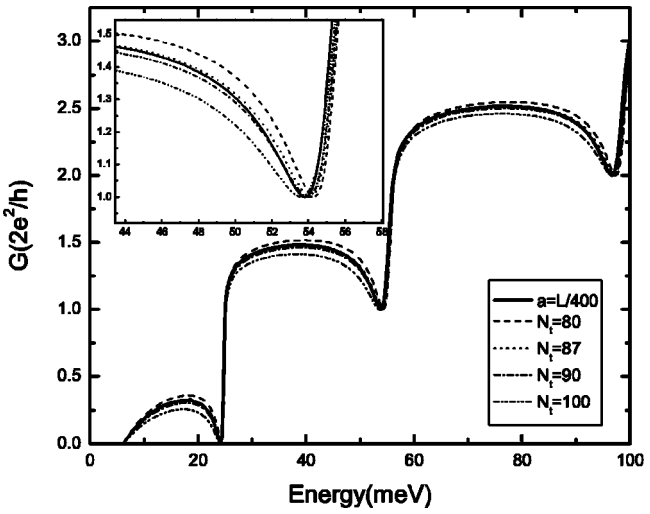

FIG. 7. Conductance for a waveguide with a single impurity. The solid line is for a disk shape impurity with $g=-7$ feV cm^2 and $a=L/400$. All other lines are for a δ-function impurity with a finite number of modes N_t and $g=-7$ feV cm^2. The inset shows the deviation in the first resonance dip.

$$G(x,y,x',y',E) = G^0(x,y,x',y',E) + \frac{V_0 G^0(x,y,0,y_0,E) G^0(0,y_0,x',y',E)}{1 - V_0 G^0(0,y_0,0,y_0,E)}, \tag{26}$$

where $G^0(x,y,x',y',E)$ is the Green's function for the free waveguide and is given by

$$G^0(x,y,x',y',E) = \frac{2}{L}\sum_{n=1}^{\infty} \sin\left(\frac{n\pi y}{L}\right)\sin\left(\frac{n\pi y'}{L}\right)\frac{2m^*}{\hbar^2}\frac{e^{ik_n|x-x'|}}{2ik_n} \tag{27}$$

(k_n is given as in Sec. IV A). The relation between the conductivity and the Green's function was derived by Fisher and Lee.[13] Using the Green's function, we first calculate a transmission matrix and then calculate the conductance. When we construct the Green's function, we keep only N_t modes. However, $(N_t\pi/L)^2$ must be larger than $2m^*E_f/\hbar^2$ where E_f is the Fermi energy so that we include all the propagating modes and at least one evanescent mode.

We again use an electron effective mass $m^*=0.067m_e$ and assume the width of the waveguide is $L=300$ Å. The δ-function impurity potential is $V_i(r)=g\delta^2(\mathbf{r})$, where g is the strength of the potential. We again choose $g=-7$ feV cm^2.

In order to determine an appropriate cut-off mode number N_t, we compare the conductance with a δ-function impurity to that for a finite range impurity which was calculated in Sec. IV C. In Fig. 7, we plot the conductance for the finite range disk potential (the solid line) which has radius $a=L/400$, and we plot the conductance for the δ-function potential with several different mode numbers N_t. We see that the conductance for the disk shape impurity and for the δ-function impurity have qualitatively the same properties, namely the reduction of conductance and the appearance of resonances. As shown in Fig. 7, the conductance for $N_t=87$ gives good agreement with the conductance of the disk shape potential.

We again define a proportionality constant, μ, similar to that in Sec. III. We can write the total number of modes N_t which gives us good approximation for the finite range impurity, in the form

$$N_t = \frac{L}{2a\mu}, \tag{28}$$

where the length scale of confinement is L instead of $2R$ and the impurity length scale is $2a$. For the disk shape impurity in a waveguide, μ is approximately 2.27. We have computed μ for different values of disk diameter $2a$ and the strength g of the potential. The results are shown in Table I. As we change the strength and diameter of the potential significantly, μ only changes slightly. If we replace the disk shape impurity potential with a square shaped impurity,

TABLE I. The constant μ for the disk shape potential, diameter $2a$ in a quantum waveguide, width L for different potential strength g and radius.

g(feV cm^2)	$2a$	N_t	μ
−7	$L/50$	23	2.17
	$L/75$	32	2.34
	$L/120$	52	2.31
	$L/200$	87	2.30
−9	$L/50$	22	2.27
	$L/100$	42	2.38
−12	$L/50$	22	2.27
	$L/120$	52	2.31

TABLE II. The constant μ for the square shape potential, width $2a$ in a quantum waveguide, width L for different potential strength g and width.

g(feV cm^2)	$2a$	N_t	μ
−7	$L/160$	60	2.67
	$L/240$	78	3.08
−9	$L/80$	30	2.67
−12	$L/160$	60	2.67
	$L/240$	78	3.08

$V_I(x,y)=g/(2a)^2$ for $0<x<2a$ and $y_0-a<y<y_0+a$, we can again compute μ. The results are shown in Table II. The value of μ is 2.67 with 15% error. Thus, the quantity μ appears to depend more on the geometry of the system than on the size or strength of the impurity.

In open systems, a δ-function impurity only allows s-wave scattering. Scattering from a finite range impurity is predominantly s-wave as long as the wave vector, k, of the incident particle and the range of the potential, a, satisfy the condition $ka \ll 1$.[14] For the calculations shown in Fig. 7, we are in a regime where only a few propagating modes contribute and $k_F a \ll 1$. This appears to be the reason that the δ-function impurity reproduces so well the conductivity for the finite range impurity, at least in regions away from the resonance. As shown in inset of Fig. 7, there is a small deviation of the resonance dip positions between the δ-function impurity (dotted line) and the finite range impurity (solid line), although the conductance plateaus have good agreement. Nevertheless the differences are small in the low energy regime. Thus, it appears that we can model a finite range impurity in a two-dimensional waveguide by using a δ-function impurity with a finite number of modes, at least as long as the condition $k_F a \ll 1$ is satisfied.

In a typical quantum point contact experiment, for example, in Ref. 1, the Fermi wavelength λ_F is 37 nm ($E_F=16$ meV). In order to satisfy the condition $k_F a \ll 1$, a should be much less than 58.89 Å. Therefore we can apply the delta function approximation for an impurity which has a radius of order of a few angstroms.

V. CONCLUSIONS

A δ-function potential in two or three space dimensions does not yield convergent expressions for bound state energies in closed systems or scattering properties in open systems. However, we find that a δ-function can be used to model a finite range potential if the number of modes used is truncated in an appropriate manner.

We have calculated the conductance for a finite range impurity in a two-dimensional waveguide by using the reaction matrix theory. We have shown that the conductance for a δ-function impurity is the same as that of a finite range impurity as long as the mode number N_t is chosen correctly and the Fermi energy is small enough.

Boese *et al.*,[4] noticed that the number of modes N_t is inversely proportional to the corresponding size of impurity by using the modified δ-function model mentioned in Sec. II. We have shown here that it is, in fact, determined by the ratio of the impurity range and the size of the confinement region and we have obtained a quantitative expression for the truncation condition.

ACKNOWLEDGMENTS

The authors thank the Robert A. Welch Foundation (Grant No. F-1051) and the Engineering Research Program of the Office of Basic Energy Sciences at the U.S. Department of Energy (Grant No. DE-FG03-94ER14465) for support of this work.

APPENDIX: THE SCATTERING MATRIX

In this Appendix, we construct the scattering matrix for an electron wave in a waveguide with a finite range impurity. Let us first substitute Eqs. (20) and (22) into Eq. (17). This gives a matrix equation which we write schematically in the following form:

$$\begin{pmatrix} \overline{A_p}-\overline{B_p} \\ -\overline{B_e} \\ \overline{C_p}-\overline{D_p} \\ -\overline{D_e} \end{pmatrix} = \overline{K}\cdot\overline{R}\cdot\overline{K}\cdot \begin{pmatrix} i(\overline{A_p}+\overline{B_p}) \\ -\overline{B_e} \\ i(\overline{C_p}+\overline{D_p}) \\ -\overline{D_e} \end{pmatrix} \tag{A1}$$

where

$$\overline{R} = \begin{pmatrix} R_{ll}(p,p) & R_{ll}(p,e) & R_{ll}(e,p) & R_{ll}(e,e) \\ R_{lr}(p,p) & R_{lr}(p,e) & R_{lr}(e,p) & R_{lr}(e,e) \\ R_{rl}(p,p) & R_{rl}(p,e) & R_{rl}(e,p) & R_{rl}(e,e) \\ R_{rr}(p,p) & R_{rr}(p,e) & R_{rr}(e,p) & R_{rr}(e,e) \end{pmatrix}, \tag{A2}$$

$$\overline{A_p} = \begin{pmatrix} a_1^p e^{ik_1 x_l} \\ \vdots \\ a_m^p e^{ik_m x_l} \end{pmatrix}, \ \overline{B_p} = \begin{pmatrix} b_1^p e^{-ik_1 x_l} \\ \vdots \\ b_m^p e^{-ik_m x_l} \end{pmatrix}, \tag{A3}$$

$$\overline{C_p} = \begin{pmatrix} c_1^p e^{-ik_1 x_r} \\ \vdots \\ c_m^p e^{-ik_m x_r} \end{pmatrix}, \ \overline{D_p} = \begin{pmatrix} d_1^p e^{ik_1 x_r} \\ \vdots \\ d_m^p e^{ik_m x_r} \end{pmatrix}, \tag{A4}$$

$$\overline{B_e} = \begin{pmatrix} b_{m+1}^p e^{\kappa_{m+1} x_l} \\ \vdots \\ b_N^p e^{\kappa_N x_l} \end{pmatrix}, \ \overline{D_e} = \begin{pmatrix} d_{m+1}^p e^{-\kappa_{m+1} x_r} \\ \vdots \\ d_N^p e^{-\kappa_N x_r} \end{pmatrix} \tag{A5}$$

and

$$\overline{K} \equiv \begin{pmatrix} \overline{K_p} & \cdots & \cdots & 0 \\ \vdots & \overline{K_e} & \ddots & \vdots \\ \vdots & \ddots & \overline{K_p} & \vdots \\ 0 & \cdots & \cdots & \overline{K_e} \end{pmatrix}, \tag{A6}$$

where $\overline{K_p}$ is a diagonal matrix with elements $\sqrt{k_n}$ ($n=1,\ldots,m$) and $\overline{K_e}$ is a diagonal matrix with elements $\sqrt{\kappa_n}$

$(n=m+1,\ldots,N)$. In these equations, the subscript p (e) denotes propagating (evanescent) modes. If we consider total N modes and there are m propagating modes for a given Fermi energy, $R_{ll}(p,p)$ is an $m\times m$ matrix, $R_{ll}(p,e)$ is an $m\times(N-m)$ matrix, $R_{ll}(e,e)$ is an $(N-m)\times(N-m)$ matrix, $\overline{K_p}$ is $m\times m$ diagonal matrix and $\overline{K_e}$ is $(N-m)\times(N-m)$ diagonal matrix.

After a lengthy linear algebra calculation, the matrices $\overline{B_e}$ and $\overline{D_e}$ which involve evanescent modes, can be expressed in terms of matrices $\overline{A_p}$, $\overline{B_p}$, $\overline{C_p}$, and $\overline{D_p}$ which involve propagating modes and we obtain the following expressions:

$$\overline{B_e} = i\overline{Q_0}\,\overline{Q_1}(\overline{A_p}+\overline{B_p}) + i\overline{Q_0}\,\overline{Q_2}(\overline{C_p}+\overline{D_p}) \tag{A7}$$

and

$$D_e = i\overline{Y}\{(\overline{K_e}R_{rl}(e,p)\overline{K_p} - \overline{K_e}R_{rl}(e,e)\overline{K_e}\,\overline{Q_0}\,\overline{Q_1})\,\overline{A_p}+\overline{B_p}) + (\overline{K_e}R_{rr}(e,p)\overline{K_p} - \overline{K_e}R_{rl}(e,e)\overline{K_e}\,\overline{Q_0}\,\overline{Q_2})(\overline{C_p}+\overline{D_p})\}, \tag{A8}$$

where

$$\overline{Q_0} = \frac{1}{\overline{K_e}R_{ll}(e,e)\overline{K_e} - \overline{K_e}R_{rl}(e,e)\overline{K_e}\,\overline{Y}\,\overline{K_e}R_{rl}(e,e)\overline{K_e} - \mathbf{1_e}}, \tag{A9}$$

$$\overline{Q_1} = \overline{K_e}R_{ll}(e,p)\overline{K_p} - \overline{K_e}R_{lr}(e,e)\overline{K_e}\,\overline{Y}\,\overline{K_e}R_{rl}(e,p)\overline{K_p}, \tag{A10}$$

$$\overline{Q_2} = \overline{K_e}R_{lr}(e,p)\overline{K_p} - \overline{K_e}R_{lr}(e,e)\overline{K_e}\,\overline{Y}\,\overline{K_e}R_{rr}(e,p)\overline{K_p}, \tag{A11}$$

$$\overline{G_1} = \overline{Y}(\overline{K_e}R_{rl}(e,p)\overline{K_p} - \overline{K_e}R_{rl}(e,e)\overline{Q_0}\,\overline{Q_1}), \tag{A12}$$

$$\overline{G_2} = \overline{Y}(\overline{K_e}R_{rr}(e,p)\overline{K_p} - \overline{K_e}R_{rl}(e,e)\overline{Q_0}\,\overline{Q_2}), \tag{A13}$$

and

$$\overline{Y} = \frac{1}{\overline{K_e}R_{rr}(e,e)\overline{K_e} - \mathbf{1_e}}. \tag{A14}$$

In the above equations, $\mathbf{1_e}$ is the $(N-m)\times(N-m)$ identity matrix. If we substitute Eqs. (A7) and (A8) into Eq. (A1), we obtain an equation relating the amplitudes of the propagating modes,

$$\begin{pmatrix} \overline{A_p} - \overline{B_p} \\ \overline{C_p} - \overline{D_p} \end{pmatrix} = i\begin{pmatrix} \overline{Z_1} & \overline{Z_2} \\ \overline{Z_3} & \overline{Z_4} \end{pmatrix}\begin{pmatrix} \overline{A_p} + \overline{B_p} \\ \overline{C_p} + \overline{D_p} \end{pmatrix}$$

where

$$\overline{Z_1} = \overline{K_p}R_{ll}(p,p)\overline{K_p} - \overline{K_p}R_{ll}(p,e)\overline{K_e}\,\overline{Q_0}\,\overline{Q_1} - \overline{K_p}R_{lr}(p,e)\overline{K_e}\,\overline{G_1}, \tag{A15}$$

$$\overline{Z_2} = \overline{K_p}R_{lr}(p,p)\overline{K_p} - \overline{K_p}R_{ll}(p,e)\overline{K_e}\,\overline{Q_0}\,\overline{Q_2} - \overline{K_p}R_{lr}(p,e)\overline{K_e}\,\overline{G_2}, \tag{A16}$$

$$\overline{Z_3} = \overline{K_p}R_{rl}(p,p)\overline{K_p} - \overline{K_p}R_{rl}(p,e)\overline{K_e}\,\overline{Q_0}\,\overline{Q_1} - \overline{K_p}R_{rl}(p,e)\overline{K_e}\,\overline{G_1}, \tag{A17}$$

$$\overline{Z_4} = \overline{K_p}R_{rr}(p,p)\overline{K_p} - \overline{K_p}R_{rl}(p,e)\overline{K_e}\,\overline{Q_0}\,\overline{Q_2} - \overline{K_p}R_{rr}(p,e)\overline{K_e}\,\overline{G_2}. \tag{A18}$$

The matrices $\overline{Z_1}-\overline{Z_4}$ are all $m\times m$ matrices.

The *scattering matrix* $\overline{\mathbf{S}}$ relates the outgoing propagating modes to the incoming propagating modes. Using Eq. (A6), we rewrite the Eq. (A15) in the form

$$\begin{pmatrix} \overline{b^p} \\ \overline{d^p} \end{pmatrix} = U^\dagger\frac{\mathbf{1_p} - i\tilde{\mathbf{Z}}}{\mathbf{1_p} + i\tilde{\mathbf{Z}}}U^\dagger\begin{pmatrix} \overline{a^p} \\ \overline{c^p} \end{pmatrix} \tag{A19}$$

where

$$\tilde{\mathbf{Z}} = \begin{pmatrix} \overline{Z_1} & \overline{Z_2} \\ \overline{Z_3} & \overline{Z_4} \end{pmatrix}.$$

The matrix $\tilde{\mathbf{Z}}$ in Eq. (A20) is a $2m\times 2m$ matrix,

$$U^\dagger = \begin{pmatrix} e^{-ik_1x_l} & & & & & & \\ & \ddots & & & & & \\ & & e^{-ik_mx_l} & & & & \\ & & & e^{-ik_1x_r} & & & \\ & & & & \ddots & & \\ & & & & & e^{-ik_mx_r}, & \end{pmatrix} \tag{A20}$$

and $\mathbf{1_p}$ is $m\times m$ identity matrix. Therefore, the scattering matrix is given by

$$\overline{\mathbf{S}} = U^\dagger\frac{\mathbf{1_p} - i\tilde{\mathbf{Z}}}{\mathbf{1_p} + i\tilde{\mathbf{Z}}}U^\dagger = \begin{pmatrix} \overline{r} & \overline{t'} \\ \overline{t} & \overline{r'} \end{pmatrix} \tag{A21}$$

where $\overline{t}$ and $\overline{t'}$ are $m\times m$ matrices of transmission probability amplitudes and $\overline{r}$ and $\overline{r'}$ are $m\times m$ matrices of reflection probability amplitudes.

[1] M. A. Topinka, B. J. LeRoy, R. M. Westervelt, S. E. J. Shaw, R. Fleischmann, E. J. Heller, K. D. Maranowski, and A. C. Gossard, Nature (London) **410**, 183 (2001).
[2] P. F. Bagwell, Phys. Rev. B **41**, 10 354 (1990); J. Phys.: Condens. Matter **2**, 6179 (1990).
[3] D. Boese, M. Lischka, and L. E. Reichl, Phys. Rev. B **61**, 5632 (2000).
[4] D. Boese, M. Lischka, and L. E. Reichl, Phys. Rev. B **62**, 16 933 (2000).
[5] K. Huang, Int. J. Mod. Phys. A **4**, 1037 (1989).
[6] M. Y. Azbel, Phys. Rev. Lett. **67**, 1787 (1991).
[7] R. Jackiw, in *M. A. B. Beg Memorial Volume*, edited by A. Ali and P. Hoodbhoy (World Scientific, Singapore, 1991).
[8] G. Akguc and L. E. Reichl, Phys. Rev. E **64**, 056221 (2001).
[9] E. P. Wigner and L. Eisenbud, Phys. Rev. **72**, 29 (1947).
[10] A. M. Lane and R. G. Thomas, Rev. Mod. Phys. **30**, 257 (1958).
[11] L. E. Reichl, *The Transition to Chaos in Classical Conservative Systems: Quantum Manifestations*, 2nd ed. (Springer-Verlag, New York, 2004).
[12] G. Akguc and L. E. Reichl, Phys. Rev. E **67**, 046202 (2003).
[13] Daniel S. Fisher and Patrick A. Lee, Phys. Rev. B **23**, 6851 (1981).
[14] Eugen Merzbacher, *Quantum Mechanics*, 2nd ed. (Wiley, New York, 1974).